Journal of South American Earth Sciences 55 (2014) 29–42

Contents lists available at ScienceDirect

Journal of South American Earth Sciences

journal homepage: www.elsevier.com/locate/jsames

Possible sources for monogenetic Pliocene–Quaternary basaltic volcanism in northern Patagonia

Gabriela I. Massaferro [a, b, *], Miguel J. Haller [b, a], Jarda Dostal [c], Zoltán Pécskay [d], Horacio Prez [b], Carlos Meister [a, b], Viviana Alric [b]

[a] Centro Nacional Patagónico, CONICET, Bvd, Brown 2915, U9120ACD Puerto Madryn, Argentina
[b] Departamento de Geología, Universidad Nacional de la Patagonia San Juan Bosco, Sede Puerto Madryn, Bvd, Brown 3051, U9120ACD Puerto Madryn, Argentina
[c] Saint Mary's University, Nova Scotia, Canada
[d] Institute of Nuclear Research of the Hungarian Academy of Sciences, H-4001 Debrecen, PO Box 51, Debrecen, Hungary

ARTICLE INFO

Article history:
Received 13 March 2014
Accepted 3 July 2014
Available online 15 July 2014

Keywords:
Basaltic volcanism
Patagonia
Petrology
Quaternary

ABSTRACT

The Pliocene- Quaternary times in Extra-Andean Patagonia are characterized by the effusion of intraplate basalts. This work is focused on those basalts outcropping between 40° and 46°S. The age of this volcanism varies between 0.23 and 5 Ma.

Based on the general geochemical characteristics, geographic distribution, and structural framework of the region, we propose that the basalts originated in response to the back arc extension that caused the thinning, doming and fracturing of the lithosphere, and extrusion of mafic magmas with a relatively primitive nature and OIB-like compositions. The geochemical characteristics allow to distinguish three types of basalts: basanites, alkaline basalts and tholeiitic basalts, each one representing different sources and percentages of partial melt and implying a heterogeneous source. A source with these characteristics could be the lithospheric mantle.

1. Introduction

The Plioene-Quaternary basalts in Northern Patagonia are distributed along a 450 km belt extending from 40°S to 46°S, located at a distance of 200–550 km away from the trench of the active subduction zone between the Farallón-Nazca and South America plates. The ages of these rocks range from 5 to 0.23 Ma (Table 1) (Bruni, 2004; Péckscay et al., 2007; Haller et al., 2009). This volcanic belt is composed of several low-volume monogenetic volcanic fields or basaltic lava flows. Some of them have been well documented while others are poorly known. Previous studies on these volcanic fields have been done mainly by Ravazzoli and Sessana (1977), Nullo (1978, 1983), Stern et al. (1990), Cucchi et al. (2001), Bruni (2004), Massaferro et al. (2006) and Pécskay et al. (2007).

In this study, we focus on the less known basalt occurrences. This paper presents field observations, data on petrography and major and trace element compositions, Sr isotopic ratios, K/Ar ages and discusses the petrogenesis of the basaltic rocks and their geodynamic significance.

Three types of volcanic centers were recognized: (1) smaller volcanic plateaus formed by the coalescence of basaltic shield volcanoes (Cerro Fermin, Crater Basalt Volcanic Field); (2) polygenic volcanic complexes and monogenetic volcanoes (Cerro Antitruz, Crater Basalt Volcanic Field, Cerro Pillahuinco Chico) and (3) cinder cones and isolated valley-filling lava flows (Cerro Horqueta, Comallo area). South of 46°S, the Quaternary Extra Andean basalts have been related to an asthenospheric slab window formed after the collision of different segments of the Chile Ridge with the subduction zone (e.g. Ramos and Kay, 1992; Gorring et al., 1997; D'Orazio et al., 2000; Gorring et al., 2003; among others). To the north, between 38°S and 39°S, there are several Plio-Pleistocene volcanic fields attributed to an extension in the back-arc caused by the steepening of the Nazca plate after a period of shallow subduction (Kay et al., 2004, 2006; Folguera et al., 2007, 2008; Søager et al., 2013). To the east, the Somuncura plateau, formed by a large volume of Tertiary volcanic rocks, is composed mainly of alkaline and tholeitic basalts. There are many hypotheses about the origin of this plateau and they will be discussed later.

* Corresponding author. Centro Nacional Patagónico, Bvd. Brown 2915, U9120ACD Puerto Madryn, Argentina. Tel.: +54 280 4451 024; fax: +54 280 4454 543.
E-mail addresses: gim@cenpat.edu.ar, gamassa2@yahoo.com.ar (G.I. Massaferro).

http://dx.doi.org/10.1016/j.jsames.2014.07.001
0895-9811/

Table 1
Whole rock K/Ar ages of Plio-Pleistocene basalts from Northern Patagonia.

Sample	Location	Latitude	Longitude	Age K/Ar	Ref
P 22	Quetrequile	−41.76585	−69.35825	1.3 ± 0.28	
P 20	Moreniyeu	−42.26238	−69.28802	1.55 ± 0.08	
PA-10	Pampa de Agnia	−43.67003	−69.88736	2.49 ± 0.1	
MS 74	Pampa de los Guanacos	−45.25665	−68.95487	2.69 ± 0.09	
MS72	Pampa de los Guanacos	−45.27492	−68.83270	2.89 ± 0.11	
P 8	Mamuel Choique	−41.53413	−70.28500	4.9 ± 0.17	
P 9	Mamuel Choique	−41.76830	−70.15598	5.65 ± 0.21	
GS 10	Río Chico	−42.05513	−70.46728	0.32 ± 0.06	Pécskay et al., 2007
GS 7	Río Chico	−42.05513	−70.46373	0.36 ± 0.13	Pécskay et al., 2007
GS 8	Río Chico	−42.05650	−70.46463	0.23 ± 0.10	Pécskay et al., 2007
GS 4	Eroded scoria cone	−42.07073	−70.16670	1.04 ± 0.43	Pécskay et al., 2007
GS 5	C. Fermín	−42.01907	−70.19487	0.58 ± 0.31	Pécskay et al., 2007
GS 6	C. Fermín	−42.01807	−70.18685	0.61 ± 0.24	Pécskay et al., 2007
PA 382	Sierra de San Bernardo	−45.45389	−69.67139	3.79 ± 0.32	Bruni 2004
PA 400	C. Grande	−45.19806	−69.97333	2.87 ± 0.68	Bruni 2004
PA 421	M. Pedrero	−45.29583	−70.20444	2.71 ± 0.10	Bruni 2004
PA 380	Sierra de San Bernardo	−45.50694	−69.34806	2.65 ± 0.14	Bruni 2004
PA 409	C. Chenques	−44.86917	−70.10806	2.49 ± 0.18	Bruni 2004
PA 406	C. Chenques	−44.87056	−70.07083	2.26 ± 0.11	Bruni 2004
PA 390	C. Ante	−44.71056	−70.77028	1.46 ± 0.20	Bruni 2004

2. Methodology

Only samples without xenoliths and xenocrysts and without alteration were analyzed. The more common and representative type of basalt was selected for each volcanic field. Whole rock major and trace elements (Table 2) were determined using lithium tetraborate fusion at the Activation Laboratories, Ancaster, Ontario, Canada. Major elements and some trace elements (V, Ni, Zn, Rb, Ba, Sr, Y, Ga, Nb, La, Ce and Zr) were determined by inductively coupled plasma-optical emission spectrometry, whereas other trace elements (REE, Th, U, Ta, Nb and Hf) were analyzed using a Perkin Elmer Optima 3000 inductively coupled plasma mass spectrometer. Based on replicate analyses, the precision is generally between 2 and 10% for trace elements and 3–5% for major elements. $^{87}Sr/^{86}Sr$ isotopic ratios of whole rocks were determined in Activation Laboratories, Ancaster, Ontario, Canada. Rb and Sr were separated using conventional cation-exchange techniques. The analyses were performed on a multi-collector mass-spectrometer (TIMS) in static mode.

K/Ar age determinations have been performed at ATOMKI, Hungary following the procedures described in Pécskay and Molnár (2002): Samples were crushed and sieved to 250-100 μm. For Ar determination a portion of sieved fraction was washed with distilled water and dried for 24 h. A portion of the whole rock sample was ground with a mortar and the powder obtained was used to analyze K and Ar. For K determination, finely ground samples were digested in acids and finally dissolved in HCl. Potassium was determined by flame photometry with a Na buffer and a Li internal standard. The measurements were checked using the inter-laboratory standards Asia 1/65 m KO-6, HD-B1 and GL-O. The analytical uncertainty is better than 2%. Argon was extracted from the samples by RF fusion in Mo crucibles. ^{39}Ar spike was added from gas pipette system and the evolved gases were cleaned using Ti and SAES getters and liquid nitrogen traps. The purified Ar was transported into the mass spectrometer and the Ar isotope ratios were measured in static mode, using a 15 cm magnetic sector type mass spectrometer.

3. Geological and structural setting

The studied area comprises the Extra Andean region of Argentina between 40° and 46°S (Fig. 1). The northern part is located between the Somuncura Massif to the east and the Precordillera Patagónica to the west, while the southern edge is located in the area of the Golfo San Jorge Basin. Within this sector, many isolated Quaternary volcanic fields or lava flows are poorly known and had been included in this work, (Fig. 2). Some of them are located about 200 km away from the present magmatic arc and 100 km from the Liquiñe-Ofqui fault zone (LOFZ), while the easternmost outcrops are nearly 550 km from the arc and 200 km from the LOFZ.

The subduction rate of the Nazca Plate is about 7–9 cm/year with an oblique component (DeMets et al., 1990; Norabuena et al., 1998) and a subduction dip angle of 15°–20° (Belmonte-Pool and Comte, 1997). The age of the oceanic subducting plate at 41°S is 15–20 Ma (Müller et al., 1997). The Liquiñe-Ofqui fault zone is a major feature of the Southern Andes developed as a consequence of the oblique subduction of the Nazca Plate beneath the South American Plate and extends from 38° to 46.5°S. It is an active dextral strike slip fault zone that comprises a set of intra arc lineaments that seem to control the Quaternary volcanoes within the arc (Cembrano and Lara, 2009).

The studied area is limited in the east by the Somuncura plateau that is a huge late Oligocene-early Miocene volcanic mainly composed of alkaline and tholeiitic basalts and minor siliceous volcanic rocks (Remesal, 1988; Kay et al., 1993; Mahlburg Kay et al., 2007 and references therein). The Paleozoic igneous metamorphic basement of the region is covered by Jurassic silicic and intermediate volcanics and Cretaceous-Tertiary sedimentary rocks. The structure in this region is controlled by extensional tectonics that formed blocks and half-grabens (Ciciarelli, 1990). The orientation of the main fractures are E–W, NE–SW and NW–SE. The Gastre (N55°W, N55°E) and Comallo (N15°W, N35°E) fault systems are interpreted by Coira et al. (1975) to be ancient basement fractures.

The western limit of the area is the Chubut Precordillera composed of Carboniferous-Early Jurassic sedimentary rocks intruded by Jurassic granitoids and covered by Tertiary volcanics.

The southern part of the study area belongs to the San Jorge Gulf Basin. This is an intracratonic extensional Cretaceous basin that underwent a tectonic inversion (Homovc et al., 1995) during the Tertiary resulting in the formation of fold structures such as the San Bernardo range. The main features that originates the basin shows an E–W orientation. During the Tertiary, profuse basaltic eruptions gave rise to the Canquel plateau that cap the San Bernardo range (Bruni et al., 2008). The basement in this area is composed of several pre Cretaceous lithologic types from Paleozoic granites, metamorphic and sedimentary rocks, Permo-Triassic igneous, sedimentary and pyroclastic rocks and middle to late Jurassic volcanic–sedimentary complexes (Sylwan, 2001).

4. General characteristics of the volcanic fields

As it was mentioned above, several small volcanic fields, lava flows or spatter/cinder monogenetic cones have been included in this work. Sampled localities include: Pampa de los Guanacos, Pampa de Agnia, Moreniyeu, Lipetrén, Mamuel Choique, Quetrequile, Huahuel Niyeu, Comallo, Cerro Horqueta, Trayén Niyeu, El

Table 2
Whole rock mayor (wt%), traces and rare earth elements (ppm) contents of the analyzed rocks.

Sample	J-5	J-8	J-16A	J-17	J-18	P-8	P-9	P-19	P-23	MS-72
Location	Lipetrén	Huahuel Niyeu	Comallo	Horqueta	Lipetren	Mamuel Choique	Mamuel Choique	Moreniyeu	Quetrequile	Guanacos
SiO_2	48.89	47.63	47.68	46.03	48.76	48.54	48.33	45.81	49.21	46.82
Al_2O_3	14.63	15.43	15.66	14.32	14.56	18.62	15.56	13.77	14.65	14.87
Fe_2O_3T	10.01	11.20	11.76	9.67	9.95	10.84	11.39	11.42	11.35	10.56
MnO	0.18	0.16	0.18	0.19	0.18	0.18	0.14	0.19	0.13	0.17
MgO	7.45	8.49	7.63	8.92	7.11	3.99	7.71	7.74	8.55	7.03
CaO	9.12	8.19	9.09	9.38	9.1	7.26	9.25	9.8	8.2	9.61
Na_2O	4.15	3.36	3.7	3.76	3.94	4.03	3.01	4.54	3.26	3.99
K_2O	1.54	1.72	1.14	3.73	1.57	2.2	1.02	1.85	1.41	2.09
TiO_2	2.55	2.10	1.95	2.02	2.59	1.80	1.50	2.81	1.87	2.89
P_2O_5	0.61	0.46	0.39	0.88	0.61	0.63	0.28	0.87	0.41	0.69
LOI	0	0	0.66	0	0.11	0.8	0.37	0.33	0	0.18
Total	99.13	98.74	99.84	98.90	98.48	98.89	98.56	99.14	99.04	98.90
Sc	20	22	20	24	19	14	24	19	18	16
V	186	216	215	256	209	175	247	241	192	302
Cr	220	260	200	250	210	20	390	200	280	180
Co	35	49	45	35	36	28	46	38	47	35
Ni	100	170	110	100	100	30	110	100	180	90
Cu	40	60	50	50	50	30	50	50	50	40
Zn	50	190	80	60	60	110	80	100	100	90
Ga	22	20	19	18	21	19	18	24	19	24
Rb	33	40	23	112	45	56	22	31	27	40
Sr	868	609	562	1166	844	916	495	1025	571	934
Y	22.7	24.2	19.2	77	22.8	27	21.3	25.9	17.4	24.9
Zr	170	228	137	389	194	236	167	253	174	304
Nb	77	33.3	21.4	78	60.4	26.2	12.4	73.1	34	63.3
Cs	0.4	0.5	0.3	3.8	0.5	1.7	0.5	0.4	0.3	0.4
Ba	407	395	330	856	425	460	334	609	388	522
La	38.9	27.8	16.8	51.3	37.1	28.4	15.6	54.7	23.6	53.9
Ce	79	53.5	36.1	115	75.9	57.2	30.7	106	46.1	107
Pr	9.41	6.65	4.59	14.7	8.96	7.37	4.02	12	5.55	12.1
Nd	39.2	26.2	20.4	64.6	37.3	29.7	18	48.1	23.4	49
Sm	8.03	5.81	4.76	15.8	7.88	6.5	4.28	9.82	5.14	9.41
Eu	2.5	1.83	1.59	3.87	2.45	2.07	1.41	2.99	1.63	2.88
Gd	6.99	5.22	4.86	14.4	7	5.92	4.41	8.4	4.77	8.22
Tb	0.99	0.84	0.72	2.42	0.96	0.91	0.72	1.17	0.76	1.12
Dy	5.22	4.53	4.01	14.2	5.13	4.99	3.96	5.99	3.92	5.74
Ho	0.89	0.87	0.74	2.93	0.89	0.94	0.79	1.01	0.7	0.96
Er	2.29	2.25	2	8.31[a]	2.27	2.52	2.14	2.51	1.78	2.38
Tm	0.306	0.306	0.267	1.28	0.302	0.373	0.302	0.317	0.224	0.301
Yb	1.76	1.91	1.73	7.39	1.76	2.34	1.96	1.82	1.44	1.68
Lu	0.219	0.256	0.214	0.986	0.219	0.324	0.283	0.21	0.196	0.206
Hf	3.8	4.7	3.2	8.9	4.4	4.6	3.4	5.2	3.9	6.6
Ta	3.32	1.73	1.32	5	3.25	1.37	0.55	4.81	1.51	4.47
Th	3.98	3.16	1.9	13.6	3.85	2.95	1.74	6.69	2.7	6.44
U	1.21	0.95	0.53	3.52	1.18	1.34	0.48	1.88	0.65	1.83
Mg#	63.00	64.00	60.00	68.00	62.00	46.00	61.00	61.00	63.00	60.00

Sample	PA-10	CUY-1	CUY-5	CUY-8	CUY-9	CUY-10	CUY-12
Location	P. de Agnia	El Cuy	El Cuy	El Cuy	El Cuy	Pillahuincó Chico	Pillahuincó Chico
SiO_2	44.89	55.07	50.58	40.89	41.65	42.15	41.58
Al_2O_3	13.99	15.18	11.86	11.55	11.67	12.13	11.26
Fe_2O_3T	10.97	8.91	10.28	13.22	13.66	13.00	13.35
MnO	0.20	0.14	0.17	0.21	0.22	0.20	0.21
MgO	9.96	6.43	11.51	9.47	9.94	10.36	10.96
CaO	9.53	8.06	12.04	11.88	11.91	11.25	11.5
Na_2O	4.19	3.65	1.96	4.65	4.69	4.16	4.82
K_2O	1.3	0.35	0.66	1.49	1.59	2.05	1.19
TiO_2	2.38	1.85	0.76	2.98	3.02	2.78	2.94
P_2O_5	0.9	0.16	0.2	1.69	1.68	1.6	1.65
LOI	0.33	0.2	0	1.14	0.89	0.21	0.51
Total	98.64	100.00	100.02	99.17	100.92	99.89	99.97
Sc	21	13	34	19	19	19	19
V	227	229	225	261	243	216	254
Cr	220	210	550	150	210	250	270
Co	32	27	22	19	34	22	24
Ni	130	100	70	60	100	90	110
Cu	30	30	60	30	40	30	30
Zn	<30	60	<30	<30	70	40	<30

(*continued on next page*)

Table 2 (*continued*)

Sample	PA-10	CUY-1	CUY-5	CUY-8	CUY-9	CUY-10	CUY-12
Location	P. de Agnia	El Cuy	El Cuy	El Cuy	El Cuy	Pillahuincó Chico	Pillahuincó Chico
Ga	18	19	9	12	20	17	16
Rb	25	9	21	24	17	43	9
Sr	999	353	690	1591	1603	1501	1460
Y	26.3	15.7	13.2	31.5	31.9	34.3	31
Zr	213	85	93	245	195	332	280
Nb	90.7	10.5	14.2	86.6	106	109	112
Cs	0.7	<0,1	0.1	0.5	0.6	0.5	0.5
Ba	646	212	291	571	960	842	485
La	63.8	7.13	12.4	92.5	93.1	83.5	89.9
Ce	120	15	26.5	172	174	159	170
Pr	13.2	2.1	3.32	19.2	19.5	17.8	19
Nd	51	11	14.6	75.8	77.6	70.8	75.6
Sm	9.61	3.81	3.19	14.4	14.5	13.8	14.4
Eu	2.82	1.43	0.922	4.38	4.41	3.95	4.31
Gd	8.02	4.37	3.02	11.5	11.8	11.4	11.6
Tb	1.09	0.64	0.43	1.55	1.57	1.55	1.51
Dy	5.78	3.42	2.63	7.51	7.75	7.83	7.36
Ho	1.01	0.59	0.49	1.23	1.24	1.32	1.23
Er	2.62	1.46	1.36	2.94	2.96	3.29	3.02
Tm	0.341	0.201	0.187	0.353	0.353	0.434	0.369
Yb	2.01	1.16	1.23	1.9	1.96	2.34	1.9
Lu	0.258	0.131	0.158	0.222	0.224	0.288	0.218
Hf	4.6	2.3	2.1	4.9	3.8	7.3	5.6
Ta	4.58	0.62	0.72	7.18	7.28	7	7.35
Th	8.08	0.65	1.31	10.7	11.2	10.8	10.7
U	1.67	0.17	0.37	2.41	2.06	3.06	2.95
Mg#	68.00	62.00	72.00	62.00	63.00	65.00	65.00

[a] Analytical error.

Cuy and Pillahuincó Chico (Fig. 2). The descriptions and ages of these fields were reported by Haller et al. (2008, 2009) and Massaferro et al. (2010).

4.1. Petrography

Most samples are porphyritic to microporphyritic dark grey/black basalts, some of which are vesicular or amygdaloidal. The dominant phenocryst is olivine, locally accompanied by clinopyroxene and plagioclase. Only in samples from the Trayén Niyeu centre is olivine absent and orthopyroxene occurs as a phenocryst phase. The olivine crystals are euhedral to subhedral, up to 2 mm in size, and commonly show iddingsitized rims. Clinopyroxene mostly occurs as subhedral crystals up to 1.25 mm in diameter and displays various colours as light green or purple in different samples. Plagioclase phenocrysts are subhedral, up to 2 mm in size.

Groundmass textures are intergranular, intersertal or less commonly hyalopilitic, composed of olivine + plagioclase + titanium bearing augite as the common mineral assemblage with apatite and Fe oxides as accessory phases. Feldspathoids also occur in the groundmass of some rocks; nepheline appears in El Cuy samples and leucite in the Cerro Horqueta rocks. Glass is present in the matrix of samples from several localities (Trayén Niyeu, Cuy, Huahuel Niyeu, Comallo, Pampa de Agnia).

Basaltic lavas from some localities, such as Crater Basalt (Massaferro et al., 2002) and those from Pampa de los Guanacos, Quetrequile, Comallo and Cerro Horqueta enclose small (few millimeters in size) ultramafic (dunites) and basement xenoliths. The basement xenoliths develop reaction rims composed of small pyroxene prisms. The basaltic rocks, particularly from the Trayen Niyeu centre contain xenocrysts of plagioclase, quartz, and pyroxene, up to 4 mm in size. Xenocrysts of plagioclase in this locality shows thick sieve texture rims and embayments.

4.2. Geochemistry

The results of the major and trace element analysis are shown in Table 2. The silica content of the rocks varies between 41 and 55 wt % and the alkalis range from 4 to 9.33% so that the samples plot in the tephrite, basanite, trachybasalt, basalt and basaltic andesite fields on a total alkali versus silica diagram (Le Bas et al., 1986) (Fig. 3). According to petrographic and chemical characteristics, the rocks have been divided into three groups: i) Alkaline basalts comprising Huahuel Niyeu, Comallo, Lipetrén, Mamuel Choique (samples P8 and P9), Quetrequile, Pampa de los Guanacos, Moreniyeu, and Pampa de Agnia localities; ii) Basanites from El Cuy (samples Cuy 8 and Cuy 9) and Pillahuincó Chico (samples Cuy 10 and Cuy 12) and iii) Subalkaline (tholeiitic) basalts: El Cuy (samples Cuy 1 and Cuy 5).

The Cerro Horqueta, a monogentic cone situated in the middle of the basement complex has different petrographic and chemical behavior than the previously mentioned groups and is analysed separately as a unique sample.

4.2.1. Alkaline basalts

The dominant rocks of the small Patagonian volcanic fields are alkaline basalts. They are either slightly silica undersaturated (nepheline normative) or saturated with normative olivine > hypersthene. Magnesium numbers (Mg# = 100*(Mg/Mg + Fe_t)) vary between 62 and 68 while Cr contents range from 180 to 280 ppm and Ni from 90 to 180 ppm. Using MgO as a differentiation index, the major elements (Fig. 4) do not show distinct trends while among trace elements (Fig. 5) Ni increases and Rb decreases with increasing abundance of MgO. The La/Yb ratios range from 9 to 32; Rb/Nb from 0.27 to 1.2; Ba/Ta from 116 to 256 and Ba/La from 9 to 19. All these ratios are higher in comparison with those of the basanites. The mantle-normalized trace element diagrams show similar but less steep patterns than the basanites

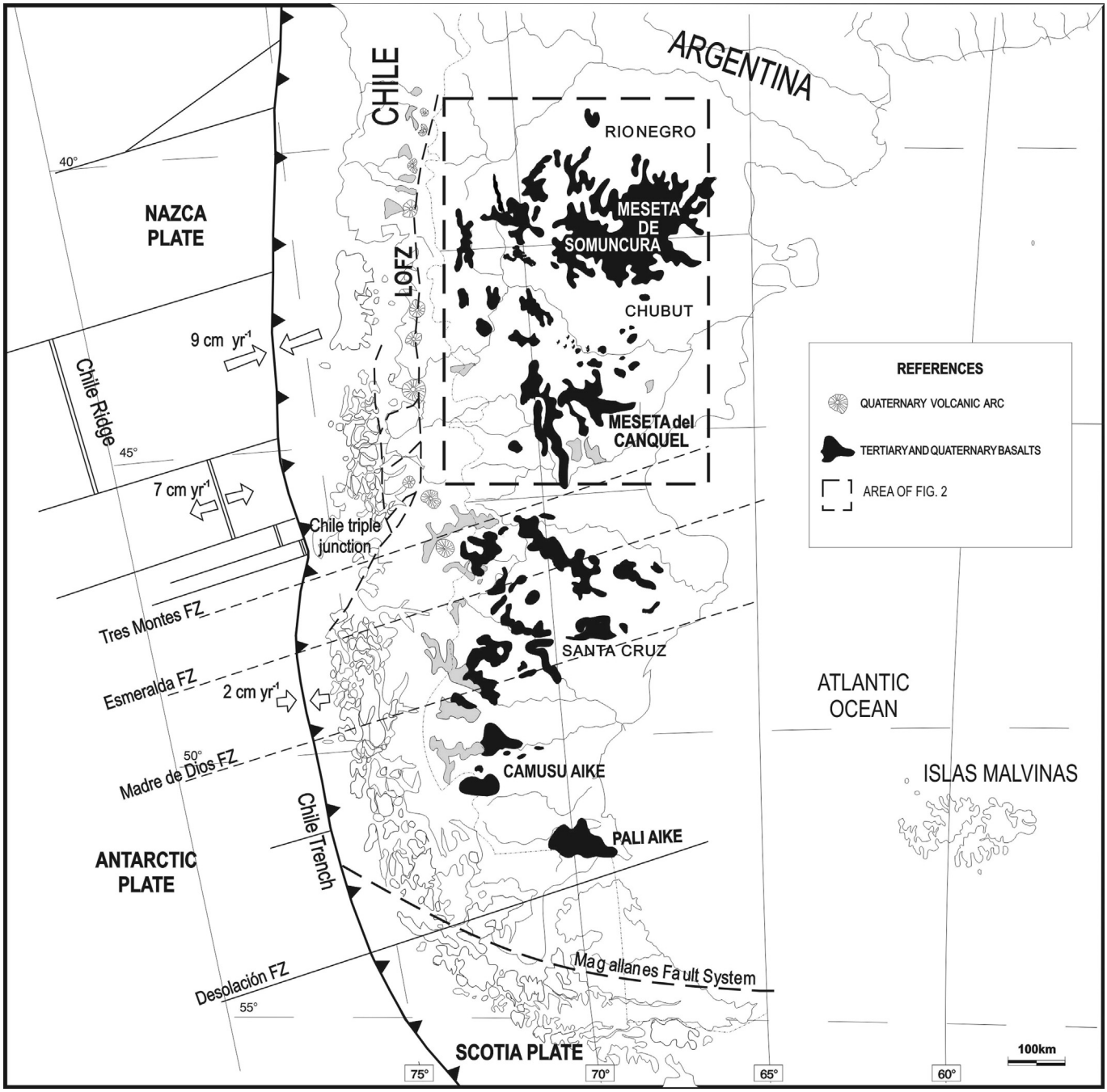

Fig. 1. Geotectonic framework of Patagonian basalts (modified from Massaferro et al., 2006).

(Fig. 6a). Sample P9 from Mamuel Choique shows a slight negative Nb–Ta anomaly and the highest Ba/La ratio.

4.2.2. Basanites

Basanites are strongly silica undersaturated rocks characterized by the presence of modal and normative nepheline. They also have low SiO_2 contents (40–42%), high Mg # (65–62) and moderate values of Cr (150–270) and Ni (60–110). In bivariate diagrams (Figs. 4 and 5), major components including $Fe_2O_3^*$, CaO, K_2O and P_2O_5 show slight decreases with increasing MgO. Among the trace elements, Ni, Nb and Cr increase while Sr decreases with higher MgO contents. This group is also characterized by the lowest Rb/Nb (0.08–0.39) and Ba/Ta (79–131) ratios. The chondrite-normalized REE patterns (Fig. 6b) are steep and smooth (La/Yb = 35–48). The trace elements plot normalized to primordial mantle (Fig. 6a) shows a smooth upward convex curve with a negative K anomaly. Samples of this group have higher LILE enrichment than the samples of the other groups analyzed (Fig. 6a).

4.2.3. Subalkaline basalts

Two samples from El Cuy (samples Cuy 1 and Cuy 5) belong to this group. They have tholeiitic affinities with high SiO_2 content so they can be classified as quartz normative basalt and basaltic andesite, respectively. Petrographically, the basaltic

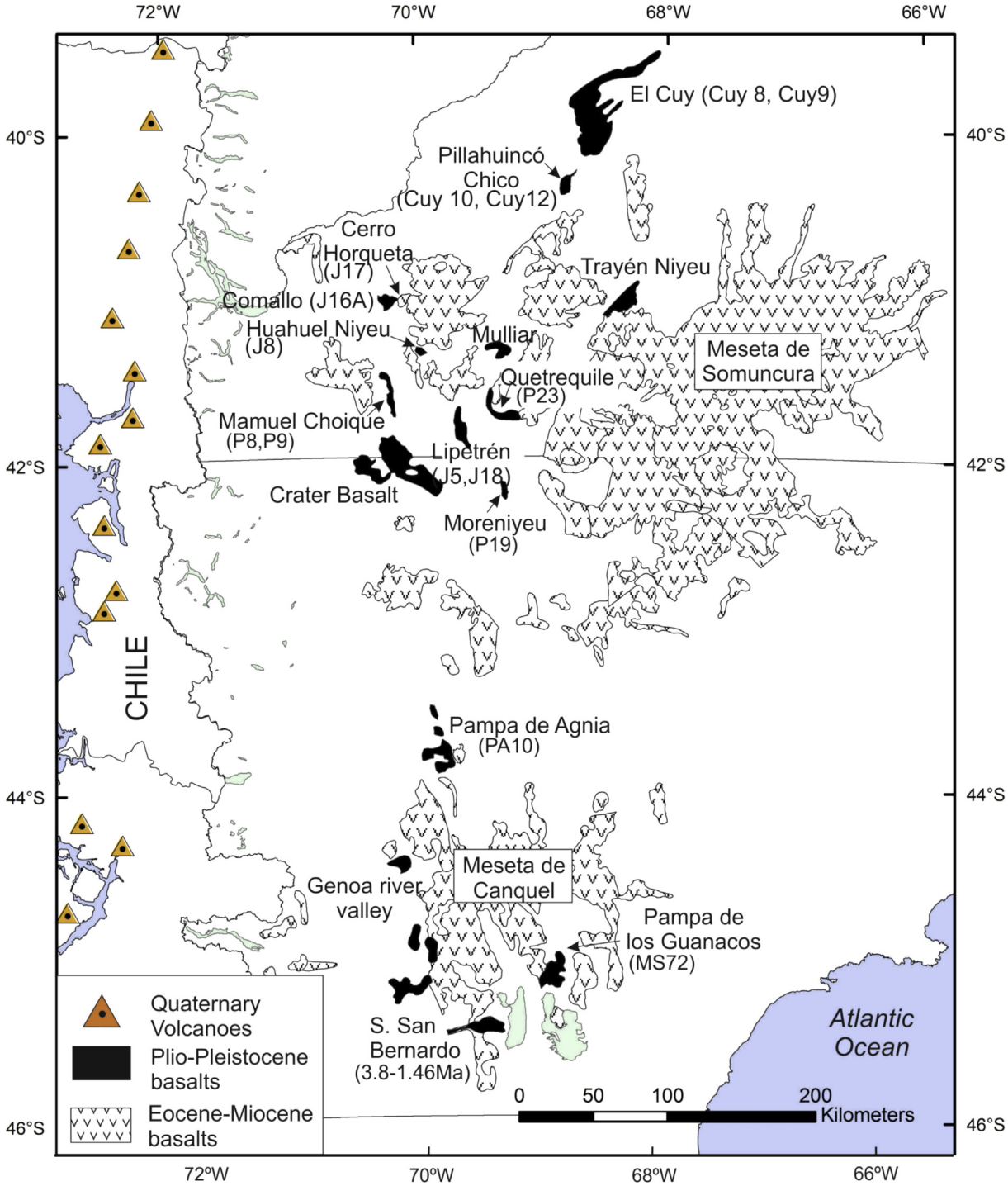

Fig. 2. Detailed location of the studied volcanic fields.

andesite (Cuy 1) has the higher proportion of plagioclase. The basaltic dike (Cuy 5) is the most primitive rock of all the studied samples, with Mg # 72 and Cr content of 550. The subalkaline basalts have Rb/Nb ratios that range from 0.8 to 1.4 and high Ba/Ta ratios (~400). The mantle-normalized trace element diagram (Fig. 6a) displays a linear, slightly LILE enriched pattern while HFSE and HREE show marked depletion with a negative slope. The patterns display distinct negative Ti and positive Rb, Ba and Sr anomalies.

4.2.4. Tephrite

The Cerro Horqueta (sample J17) composition is different from the other three groups and corresponds to tephrite on the TAS diagram (Fig. 3). It is strongly silica-undersaturated characterized by the presence of leucite in the groundmass, Mg # 68, Cr contents of 250 ppm and Ni of 100 ppm. Even though it is enriched in REE and trace elements relative to the mantle, the chondrite-normalized REE pattern (Fig. 6c) is flat with a gentle negative slope (La/Yb = 6). The Rb/Nb ratio is 1.4 and Ba/Ta = 171.

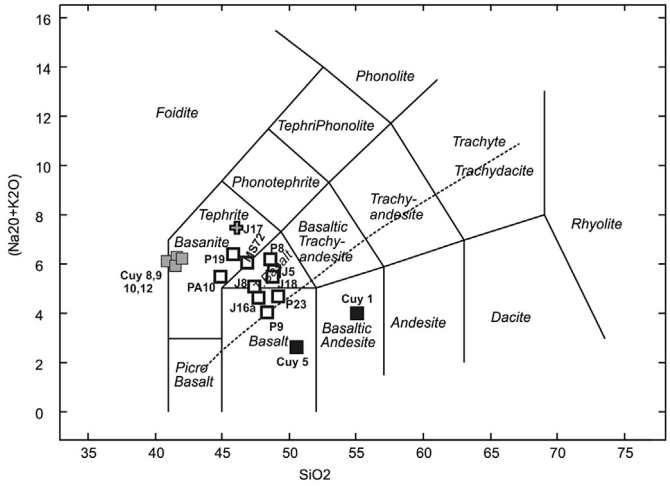

Fig. 3. TAS classification diagram from Le Bas et al. (1986). The dash line that separates alkaline from subalkaline fields is from Irvine and Baragar (1971). Light filled squares, basanites. Empty squares, alkaline basalts. Dark filled squares, subalkaline basalts. Cross, C° Horqueta.

5. Discussion

5.1. Petrogenesis

5.1.1. Basanites (samples Pillahuincó Chico, Cuy 8 and Cuy 9)

The high Mg#, Cr and Ni contents point out a relatively primitive nature for these rocks, even though the decrease of these elements with decreasing MgO implies some crystal fractionation of olivine. The decrease in Ni/Sc ratios with differentiation rules out clinopyroxene fractionation .The primitive mantle-normalized trace element patterns (Fig. 6a) show incompatible elements enrichment (with a minor positive spike at Nb–Ta) and depletion in HREE, shapes typical of intraplate alkaline basalts. The enrichment in LREE could be the result of low degrees of partial melting of a garnet-bearing source. This is also suggested by the high La/Yb (35–49) ratios and the low HREE contents. The low values of Ba/La (5–10), typical of OIB (Hickey et al., 1986) (Fig. 7) negates a role of the subducting slab fluids. As Rb is considered an element abundant in the crust and the arc magmas are depleted in Nb and enriched in Ba, a low Rb/Nb (0.08–0.39) and Ba/Nb (<10) ratios imply that the rocks were not modified by crustal contamination. The negative anomalies of K on the mantle-normalized plots (Fig. 6a) together with the low values of Rb would indicate an amphibole/phlogopite residue in the mantle. These minerals are considered to be the indicators of mantle metasomatism. Several authors have previously invoked the existence of metasomatism in the Patagonian mantle (Gorring and Kay, 2000; Aliani et al., 2004; Rivalentti et al., 2004; Bjerg et al., 2009; among others).

5.1.2. Alkaline basalts

The variable degrees of the LREE and LILE enrichment and the HREE and HFSE depletion (Fig. 6a and b) also point out an OIB like garnet source with minor input from subducted slab fluids. Patterns are comparable to those of the Crater Basalt Volcanic Field (Massaferro et al., 2006) or post plateau (Miocene) Somun Cura basalts (Mahlburg Kay et al., 2007). Even though the majority of the analyzed samples have Ba/La <20 and Ba/Nb < 10, typical of intraplate basalts, some others (Mamuel Choique, Comallo, Huahuel Niyeu and Quetrequile) have higher ratios suggesting a minor input of subducting plate fluids. Mamuel Choique sample P8 is the most affected by this slab input with the highest Ba/Ta ratios (Fig. 7), consistent with a slight negative anomaly in Nb–Ta. This could be related with a source modified by the Paleogene subduction given its western position relative to the other samples (Figs. 2 and 9). On the other hand, P8 and P9 are the older samples of the set, in the limit between Miocene and Pliocene. As was noted by Stern et al. (1990) the western Pliocene to Quaternary flows in Patagonian plateau shows arc like Ba/La and La/Ta ratios. They considered that this feature is the result of a sub arc type enrichment processes affecting the mantle source earlier in the Cenozoic.

5.1.3. Subalkaline rocks

The shape of the mantle normalized pattern of the subalkaline rocks (Fig. 6a) reflects a greater degree of partial melting in comparison with the other groups. The low Yb abundances (mantle-normalized value < 10) indicate the existence of garnet as a residual phase in the mantle. The geochemical characteristics of these rocks including the high Ba/La (>20) and Ba/Nb (~ 20) ratios suggest interaction with subducting slab fluids. Also in this case, the source of these rocks could imply a lithospheric mantle enriched by the Paleogene subduction.

The Cerro Horqueta is an isolated volcano located on a crystalline basement domain. It is the only sample without depletion in HREE and HFSE (Fig. 6c). The enrichment in Yb suggests the absence of garnet in the source. The negative anomaly at Ti indicates the presence of a residual phase in the mantle that concentrates this element, probably titanite or ilmenite. There is no evidence of magma interaction with arc materials. The Ba/Ta ratios are similar to OIB (Fig. 7), but the relatively high Rb/Nb ratio suggests crust contamination. This is supported by the quartz xenocrysts content of the sample. This basaltic rock was derived from a spinel peridotite source, at a shallower depth (Fig. 8).

Fig. 9 depicts the increase of the Ba/La ratios in the basaltic rocks towards the present arc. For the same longitude, the outcrops from the south and middle parts of the studied region have similar characteristics, while basalts from Cuy and Pillahuincó Chico do not lie on the trend. They differ from the other basalts by a different degree of melting and by the extent of crustal contamination.

Most basaltic rocks were generated at a depth greater than 70 km, in the garnet stability field (Fig. 8) as indicated by fractionated HREE and the relatively low Al_2O_3 contents (Green, 1970; Wyllie, 1981) within a relatively thinned lithosphere environment (Tassara and Yañez, 2003; Tašárová, 2007). The geotherm calculated by Bjerg et al. (2009) for the Prahuaniyeu xenoliths indicates a high heat flow for this region (between 80 and 100 mW/m^2). At a depth of 70 km, this geotherm intersects the garnet–spinel equilibrium boundary at about 1100 and 1200 °C (Bjerg et al., 2009). As these temperatures are too high for intracratonic settings, Bjerg et al. (2009) proposed the existence of a plume or plume-like component in this area in agreement with Mahlburg Kay et al. (2007).

5.2. Isotopic characteristics

Five samples from different outcrops were selected to determine the K/Ar ages. The results are reported in Table 1. The Miocene-Pliocene to Quaternary age given previously by stratigraphic and morphologic characteristics were confirmed (Nullo, 1978; Ravazzoli and Sessana, 1977; González et al., 2003). Considering the ages reported by Pécskay et al. (2007) for the Gastre volcanic field, the volcanic episode extends from 5.65 to 0.23 Ma.

Two samples without xenoliths were selected for analyses of the $^{86}Sr/^{87}Sr$ ratios from the Comallo area (sample J16a) and the other from the Huahuel Niyeu (sample J8); both samples belong to the alkaline basalts group. One value of $^{86}Sr/^{87}Sr$ for a Comallo flow is given by Stern et al. (1990) and is in accordance with those obtained

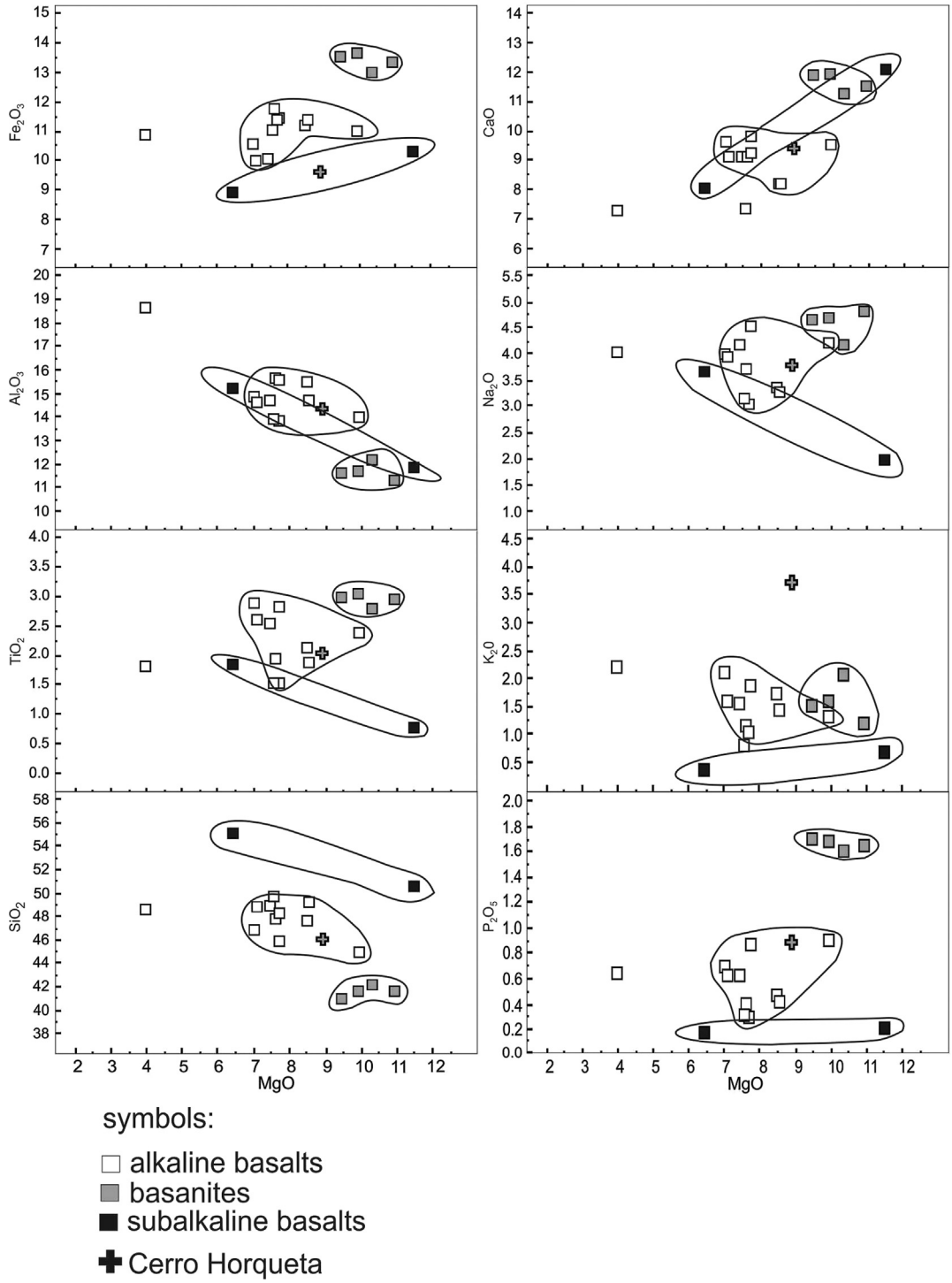

Fig. 4. MgO (wt%) vs major elements (wt%) for the three groups of basalts. Light filled squares, basanites. Empty squares, alkaline basalts. Dark filled squares, subalkaline basalts. Cross, C° Horqueta.

in this work (Table 3). The values are according to those for the mantle which implies that the source of basalts is located in the mantle. The ratios are comparable to the other Quaternary Patagonian basalts (Fig. 10), and are within the range of OIB (Hickey et al., 1986). The values are near to those for an EM1 type reservoir and the bulk earth composition (Zindler and Hart, 1986 review). Following Zindler and Hart (1986), the EM character reflects the enriched lithospheric sources.

5.3. Partial melting and source characteristics

Although the basanites have relatively high Mg# (62–65), they are not primary magmas and thus in order to calculate the degree of partial melting, it is necessary to correct the compositions for the effect of crystal fractionation. The following assumptions were made to perform the calculations: olivine is the only crystallizing phase as it was shown by the Ni and Cr decrease with decreasing

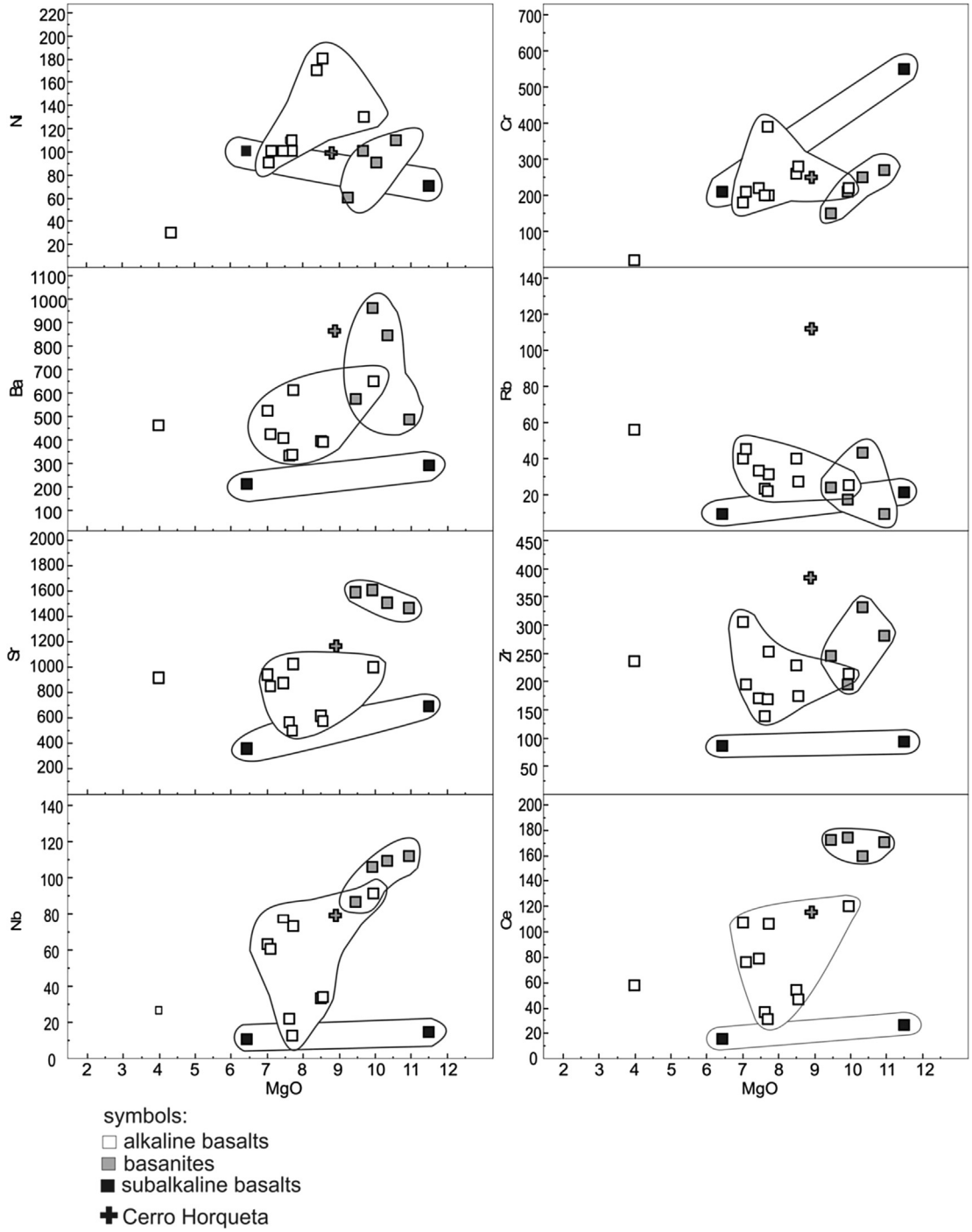

Fig. 5. MgO (wt%) vs trace elements (ppm) for the three groups of basalts. Light filled squares, basanites. Empty squares, alkaline basalts. Dark filled squares, subalkaline basalts. Cross, C° Horqueta.

MgO (Fig. 5); the Kd $(Fe/Mg)^{ol/liq}$ is constant and equal to 0,30 (Takahashi and Kushiro, 1983). Following Pearce (1978) method, olivine was added in small increments to the magma, a new composition was recalculated in each step until it arrived at a composition in equilibrium with mantle olivine (Fo_{90}) reaching a Mg# = 73.

The results show that the basanites like Cuy 12 (Table 4) or Cuy 8 needs 14% of olivine to reach primary compositions. Mass balance of major elements were performed with XLFRAC software (Stormer and Nicholls, 1978) considering non-modal batch melting starting from a moderately enriched peridotite (Chen, 1971) and the phase compositions of Table 4 to obtain the weight percent of these mineral phases in the peridotite (source). As was shown in Fig. 6, the depletion in Yb and Lu relative to the mantle, suggest that garnet should be considered as a residual phase in the source. Starting from the calculated peridotite, then another mass balance was performed to calculate the percentage of partial melting needed to reach the compositions of the primary magmas. The results indicate 1.5% of partial melting. If a hydrous source is considered, because of the possible existence of amphibole or

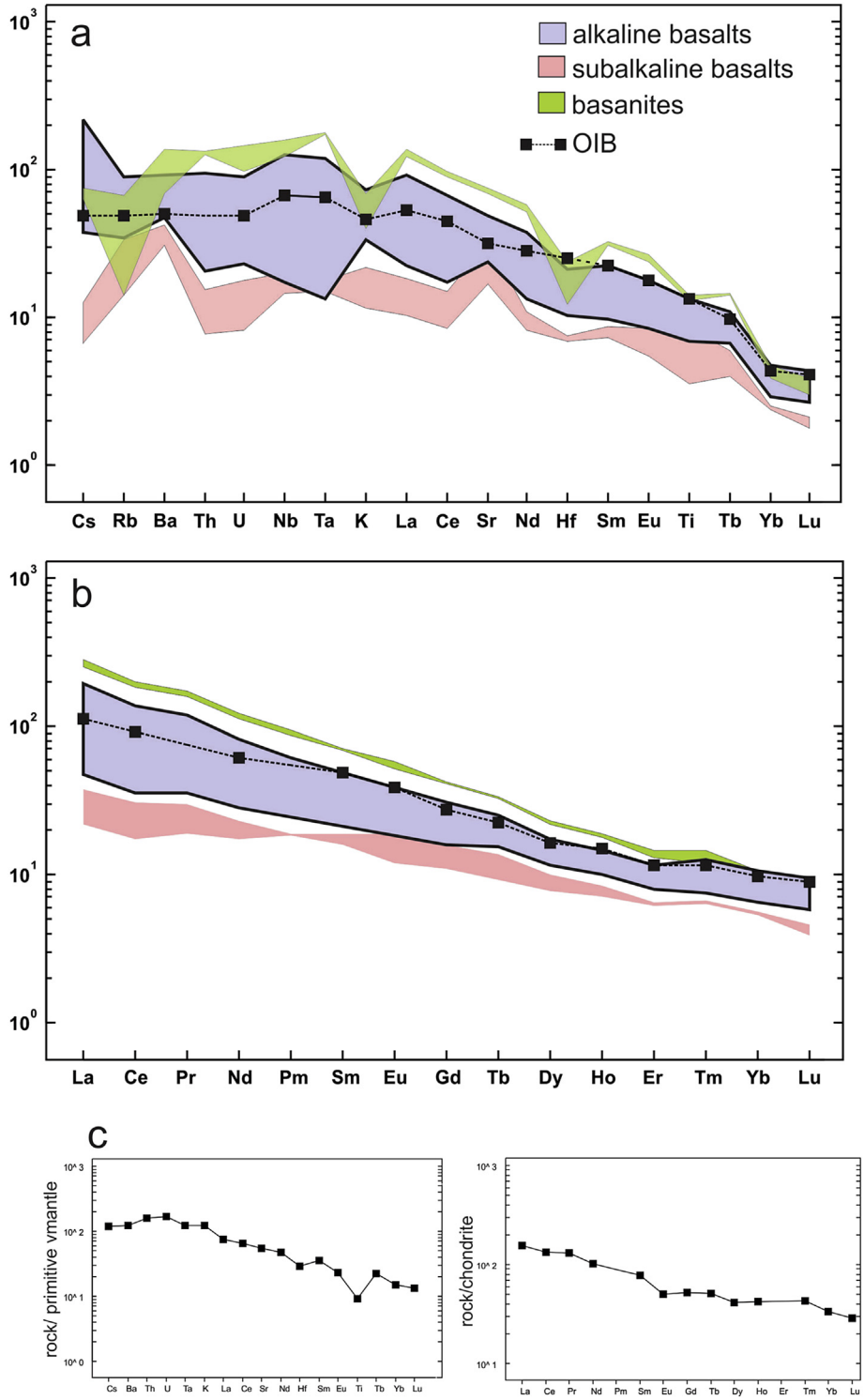

Fig. 6. a) Trace elements normalized to primitive mantle following Sun and McDonough (1989). b) REE normalized to Chondrite following Nakamura (1974). c) Trace elements and REE of sample J17 (Cerro Horqueta) with same normalizing values than in a and b. OIB contents from Sun and McDonough (1989).

phlogopite in the source (as the spikes in K and Rb suggest in the Fig. 6a), the melting degree result slightly increases to 1.7% (Table 5). Alkaline basalts require the addition of olivine between 9 and 17% (samples PA10 and P9) to reach primary magma composition (Table 4). Considering an anhydrous garnet peridotite source (Chen, 1971), the model calculations yield 2.4% and 3.7% of partial melting (samples PA10 and P9 respectively). For sample Cuy 5 (subalkaline tholeitic basalt) Mg# = 72, calculations indicate 5.3% of partial melting from an anhydrous garnet peridotite (Chen, 1971).

If the mantle source was an enriched peridotite such as the pyrolite of Ringwood (1966) the degree of partial melting would increase to 5.9% for basanites, from 8 to 10% for alkaline basalts and 8% for subalkaline basalts.

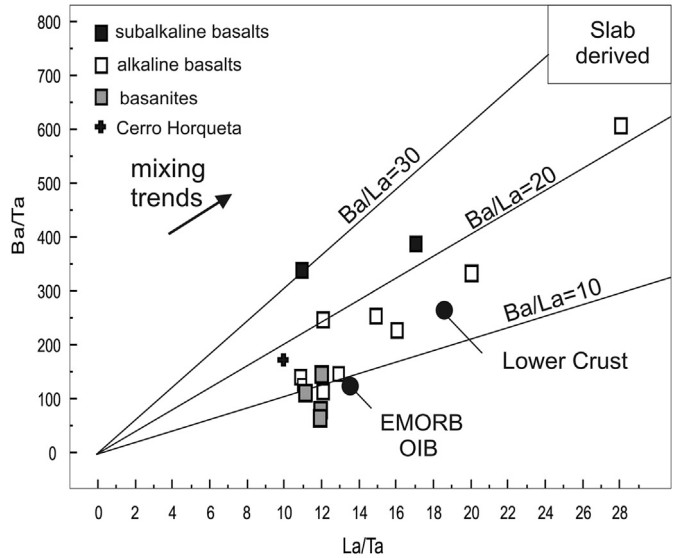

Fig. 7. Ba/Ta vs. La/Ta diagram modified from Mahlburg Kay et al. (2007).

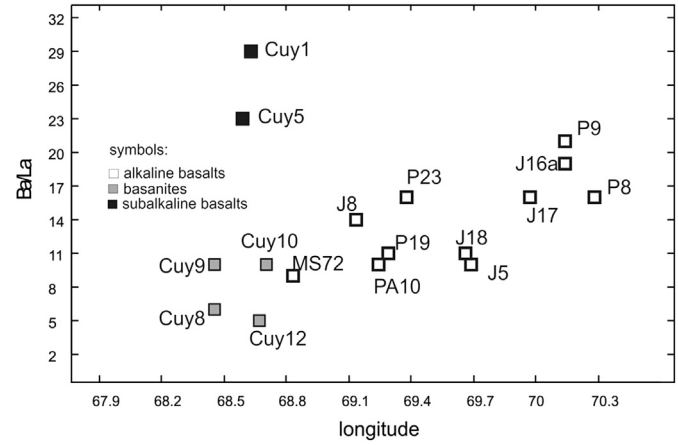

Fig. 9. Ba/La vs longitude showing the increase of this relationship towards the west, except for Cuy 1 and 5, see text for explanation. Light filled squares, basanites. Empty squares, alkaline basalts. Dark filled squares, subalkaline basalts.

The incompatible trace element concentrations of the peridotitic sources were calculated assuming batch melting (Hanson, 1978) of garnet lherzolite (Chen, 1971). The partition coefficients are from White (2013) and references therein, and McKenzie and O'Nions (1991). The melting degrees and peridotite residua were calculated with an XLFRAC program (Stormer and Nicholls, 1978) (Table 5). The normalized concentrations of incompatible trace elements of the sources for each group are shown in Fig. 11. The source of sample Cuy 12 (representative of basanites) is enriched in LILE (except Rb and K) compared to primordial mantle. Both hydrous and anhydrous peridotites were considered but in each case the negative anomalies in K and Rb remained indicating that these anomalies may be features characteristic of the source. The source for sample P9 (alkaline basalts) shows a slight depletion of trace elements except in Rb, Ba, K and Sr. The sample Cuy 5 (subalkaline basalts) source also shows HFSE depletion and slight enrichment in LILE. These differences point out different mantle sources involved in the genesis of these basalts. Such kind of heterogeneities would imply the participation of lithospheric mantle melts in the genesis of the basalts. The enrichment in the basanite source could be explained by previous metasomatic processes.

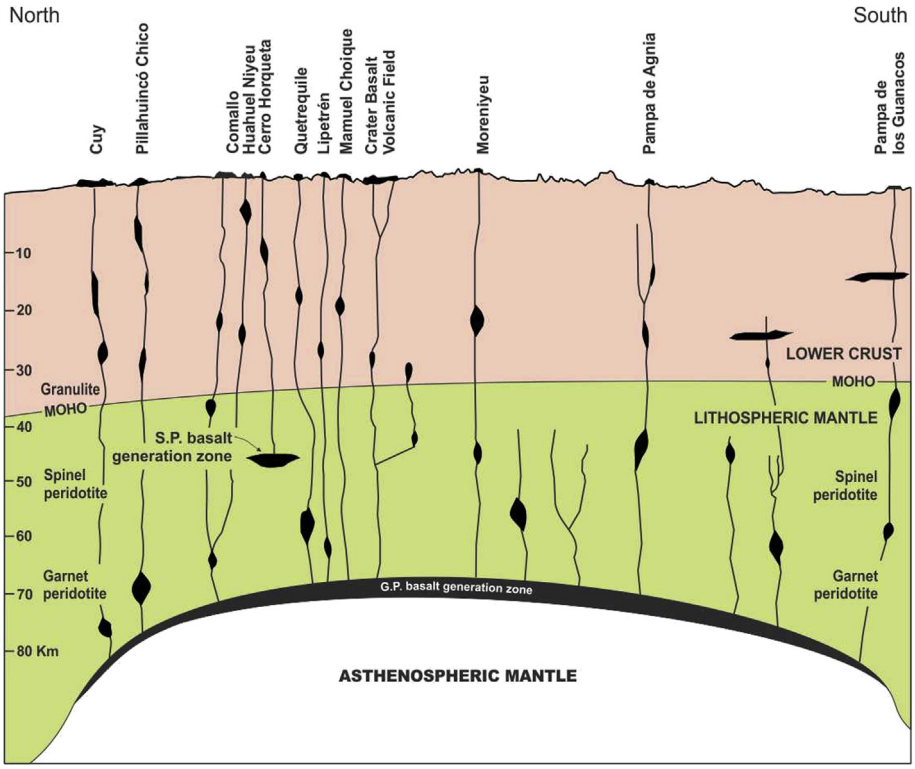

Fig. 8. Idealized North-to-South cross section of northern Patagonia, showing inferred subcrustal relations. Black shapes defining regions of magma generations do not define shapes of individual magma bodies, which are unknown and probably much more complex. S.P. = Spinel peridotite. G.P. = Garnet peridotite. Crust thickness after Tassara and Yañez (2003). Garnet peridotite depth discussed in text.

Table 3
Whole rock $^{87}Sr/^{86}Sr$ ratios of samples of Huahuel Niyeu (J8), Comallo (J16a) and C from Comallo (Stern et al., 1990).

Sample	$^{87}Sr/^{86}Sr$	±2 s
J8	0.704469	0.000017
J16a	0.704385	0.000010
C	0.70423	

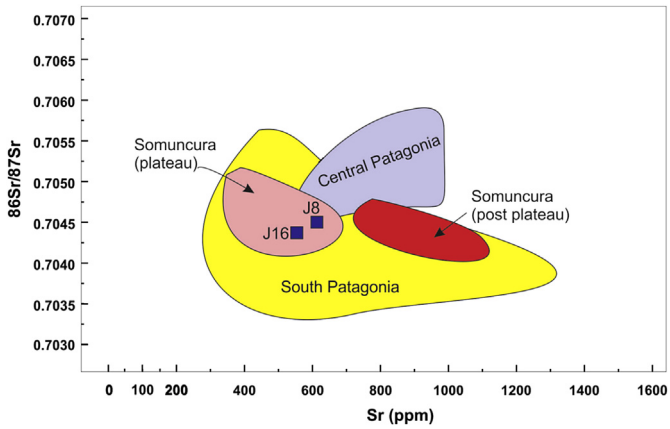

Fig. 10. Sr (ppm). vs $^{86}Sr/^{87}Sr$ for different volcanic fields of Patagonia. Data of Somuncura from Mahlburg Kay et al. (2007), South Patagonia from Gorring and Kay (2001), Central Patagonia from Bruni (2004), J16 (Comallo) and J18 (Lipetrén) belong to this study.

5.4. Geodynamic considerations

The mantle-normalized trace element patterns of almost the alkaline basalts and basanits (Fig. 6a) are comparable to an OIB-like basalt (values considered from Sun and McDonough, 1989). They show a smooth convex curve that reflects enrichment in incompatible elements in relation to the less incompatible ones. They also have low Ba/La (5–21), Rb/Nb (0.08–2.13), Th/La (0.10–0.13) and values of $^{87}Sr/^{86}Sr$ (0.704469, 0.704385) consistent with an OIB. In the chondrite normalized diagram (Fig. 6b) they have a steep rectilineous patterns with La/Yb = 7–48 (mostly >20)The low Th/La, Rb/Nb low Ba/Ta ratios indicate the lack of crustal contamination or interaction with the subducting slab fluids, with the exception of Cerro Horqueta. Additionally, the $^{87}Sr/^{86}Sr$ values are comparable to other Patagonian uncontaminated basalts (Fig. 10). As three different sources have been determined by modeling for contemporaneous and spatially associated basalts, a heterogeneous lithospheric mantle source is proposed. Partial melting of lithospheric mantle would give rise to the three different groups of basalts studied here. The OIB signature, the lack of contamination, and the presence of mantle xenoliths suggest an extensional tectonic regime for these basalts but the origin for the Cenozoic back arc volcanism in Northern Patagonia is still a matter of debate.

It has been suggested that during the Tertiary, the tectonic arrangement of the Nazca and South American plates underwent a readjustment that triggered an increase in the rate of convergence and a change from oblique to near normal convergence (Cande and Leslie, 1986; Somoza, 1998). As proposed by many authors (Muñoz et al., 2000; de Ignacio et al., 2001; Kay and Copeland, 2006; Kay et al., 2006) during Oligocene, the drastic changes in the convergence rate initiated the roll back of the Farallón-Nazca plate. Muñoz et al. (2000) suggest that the increase in the rate of convergence favored extension and slab roll back processes and the formation of a slab window from Late Oligocene to Early Miocene, while de Ignacio et al. (2001) argued that the asthenospheric upwelling was favored by a concave up geometry of the subducting plate. On the other hand, Mahlburg Kay et al. (2007) propose the existence of a plume-like mantle upwelling attributed to mantle thermal instabilities related with the plate reorganization. In this model the melting was facilitated by the hydration of the mantle during Paleogene subduction. The high heat flow postulated by Bjerg et al. (2009) favors the existence of a mantle plume- like anomaly during the Tertiary. Kay and Copeland (2006) explain the extension regime between 24 and 20 Ma. as a result of the eastward migration of the South American plate over the mantle. Bruni et al. (2008) give a similar explanation for the Eocene-Pleistocene volcanism of the Valle del Río Genoa-Sierra de San Bernardo area. The westward drift of the mantle wedge of the South American plate relative to the eastward drift of the mantle is compensated by the

Table 5
Residual peridotites after extraction of the primary magmas, considering initial Chen's peridotite composition.

Phases wt%	P1 p/Cuy 12	P2 p/Cuy 12	P p/PA10	p9	Cuy 5
ol (1)	64.09	64.07	64.09	67.36	69.27
opx (2)	20.67	20.7	20.67	20.57	20.5
cpx (3)	9.74	9.39	9.74	9.04	7.6
gr (2)	5.5	5.03	5.5	3.03	2.63
parg (4)	–	0.81	–	–	–
Total	100	100	100	100	100
r2	0.0313	0.02	0.0278	0.028	0.0285
F%	1.5	1.69	2.37	3.68	5.27

R2 = sum of cuadratic residue; F%: percent of partial fusion.

Table 4
Compositions of peridotite, phases and primary magmas use to model partial fusion. (p) = calculated primary magma; Peridotite 1 = Chen (1971); Peridotite 2 = Ringwood (1966); %ol = percentage of added olivine to reach primary composition. ol (1) = olivine from De Min (1993); opx (2) = ortopyroxene from MacGregor (1974); cpx (3) = clipyroxene from Bristow (1984); gr (2) = garnet from MacGregor (1974).

Oxides	Peridotite 1	Peridotite 2	ol (1)	opx (2)	cpx (3)	Gr (2)	parg (4)	Cuy 12 (p)	PA10 (p)	P9 (p)	Cuy 5
SiO_2	44.95	45.5	40.43	57.43	53.14	42.17	43.98	42.08	45.66	48.37	50.58
TiO_2	0.1	0.71	0.1	0.28	0.49	0.3	0.74	2.62	2.24	1.32	0.762
Al_2O_3	1.57	3.56	0.1	0.99	2.48	20.62	14.1	10.06	13.2	13.7	11.86
FeOT	8.48	8.53	9.42	6.43	4.86	12.45	3.9	12.09	10.22	10.62	9.25
MnO	0.13	0.14	0.1	0.02	0.02	0.3	0.07	0.18	0.19	0.12	0.17
MgO	40.3	37.75	48.23	33.63	16.7	18.51	17.99	15.81	13.44	13.9	11.51
CaO	2.49	3.1	0.15	0.94	20.75	4.46	10.75	10.28	8.99	8.14	12.04
Na_2O	0.35	0.57	0	0.26	1.01	0.79	3.48	4.3	3.95	2.65	1.96
K_2O	0.09	0.13	0	0	0	0.4	0.53	1.06	1.22	0.89	0.66
P_2O_5	0	0	0	0	0	0	0	1.47	0.84	0.24	0.2
Total	98.46	99.99	98.53	99.98	99.45	100	95.54	99.95	99.95	100	98.99
Mg#								73	73	73	72
% ol								14	9	17	0

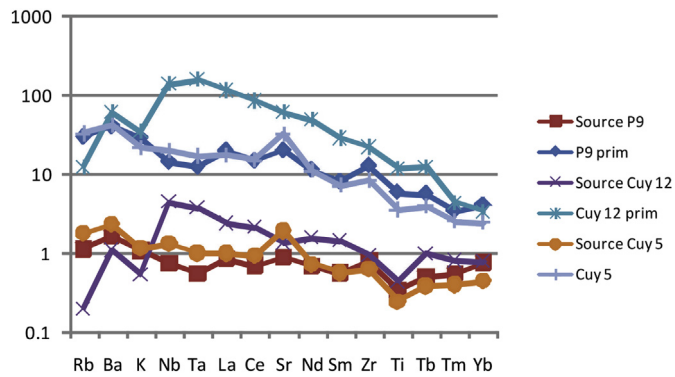

Fig. 11. Calculated source compositions for basanites (Cuy 12), alkaline (P9) and subalkaline (Cuy5) basalts normalized to primitive mantle (Sun and McDonough, 1989) and calculated primitive basalt compositions from Table 4.

asthenosphere upwelling and decompression. With time, the lithosphere is eroded and melted by the upwelling asthenosphere. Another explanation is given by Remesal et al. (2012) which involves lithospheric delamination. Zaffarana et al. (2012) consider that the shear driven upwelling process (Conrad et al., 2010) is a possible mechanism to explain the genesis of the back arc to intraplate Patagonian basalts from the Cretaceous to Cenozoic times. Aragón et al. (2011, 2013) argue the collision of the paleogene Farallon-Aluk ridge with the consecuently detachment and sinking of the Aluk plate producing the opening of a slab window that lasted 30 Ma. During this slab window the Patagonian Massif, a crustal block in the former back arc, was only affected by uplift and after that, the intraplate basalts of Sumuncura Plateau were spilt.

Kay et al. (2004) consider that the small volume Plio-Pleistocene plateau flows located south of 38° S are related to localized extension along transpresssional fault systems like LOFZ. According to these authors (Kay et al., 2004) there is no evidence of substantial extension to produce the large amount of Patagonian plateau basalts but, with a previously heated mantle, small amounts of extension could trigger mantle melting.

Within this framework of Tertiary volcanism, one way to explain the volcanism discussed in this paper is that the roll back process invoked by many authors for the Tertiary continued during the Plio-Pleistocene as was suggested by Lin (2014). The continuation of the roll back caused by the steepening of the Nazca plate below the South American Plate, could have triggered the westward migration of the volcanism during the Neogene generating basalts with similar characteristics to the Oligocene-Miocene ones but in lesser volumes.

6. Conclusions

The back arc region between 40° and 46° S in Patagonia is characterized by the presence of small-volume basaltic lava flows, monogenetic volcanic fields and scoria cones with ages varying between 5.65 and 0.23 Ma. This magmatism shows characteristics (a relative primitive nature with OIB-like compositions) similar to the southern Patagonia counterparts (e. g., Pali Aike, Glenn Cross, Meseta de la Muerte, etc) but they are not related to slab window processes. Based on petrographic and chemical characteristics the basaltic rocks can be divided into three groups: basanites, alkaline basalts, and subalkaline basalts. The geochemistry points out different sources for each group. Basanites would result from 1.5% of partial melting of an enriched garnet peridotite while the alkaline and subalkaline basalts would imply higher partial melting percentages (2% and 5% respectively) from slightly depleted anhydrous garnet sources. These sources would be located at a depth of 70 km or more within the lithospheric mantle. The difference in trace elements between each group reflects heterogeneous mantle sources. For the alkaline basalts there is an increase in the Ba/La ratios westward, which is consistent with some interaction with the subduction-related components in the lithospheric source as we approach the arc.

Small amounts of extension, related to slab roll back processes would promote asthenospheric upwelling and melting of the lithosphere mantle to give rise to this volcanism.

Acknowledgements

The authors are indebted to Dr. Silvia L. Lagorio and Dr. Gustavo W. Bertotto for their helpful suggestions and revision of the manuscript. To the Science and Technical Secretary of the Universidad Nacional de la Patagonia San Juan Bosco (PI 819) and CONICET (PIP 11220080102084) for providing funds to carry out the research project. The authors would like to thank S. Kay for her manuscript review and valuable comments.

References

Aliani, P.A., Bjerg, E.A., Ntaflos, Th, 2004. Evidencias de metasomatismo en el manto sublitosférico de Patagonia. Rev. la Asoc. Geológica Argent. 59 (4), 539–555.
Aragón, E., D'Eramo, F., Castro, A., Pinotti, L., Brunelli, D., Rabbia, O., Rivalenti, G., Varela, R., Spakman, W., Demartis, M., Cavarozzi, C., Aguilera, Y., Mazzucchelli, M., Ribot, A., 2011. Tectono-magmatic response to mayor convergence changes in the North Patagonian suprasubduction system; the Paleogene subduction-transcurrent plate margin transition. Tectonophysics 509, 218–237.
Aragón, E., Pinotti, L., D'Eramo, F., Castro, A., Rabbia, O., Coniglio, J., Demartis, M., Hernando, I., Cavarozzi, C., Aguilera, Y., 2013. The Farallon-Aluk ridge collision with South America: implications for the geochemical changes of slab window magmas from fore- to back-arc. Geosci. Front. 4 (4), 377–388.
Belmonte-Pool, A., Comte, D., 1997. Análisis del contacto sismogénico interplaca a lo largo de Chile. 8° Congreso Geológico Chileno. Actas 3, 1746–1750.
Bjerg, E., Ntaflos, T., Thoni, M., Aliani, P., Labudia, C., 2009. Heterogeneous lithospheric mantle beneath Northern Patagonia: evidence from prahuaniyeu garnet- and spinel-peridotites. J. Petrol. 50 (7), 1267–1298.
Bristow, J.K., 1984. Picritic rocks of the North Lebombo and South-East Zimbabwe. Geol. Soc. South-Africa 13, 105–123 (Special Publication).
Bruni, S., 2004. Le rocce ignee della Valle del Río Genoa-Senguerr e della catena del Cerro San Bernardo, Chubut, Argentina. University of Pisa, Italy, p. 154. PhD. Thesis.
Bruni, S., D'Orazio, M., Haller, M.J., Innocenti, F., Manetti, P., Pécskay, Z., Tonarini, S., 2008. Time-evolution of magma sources in a continental back-arc setting: the Cenozoic basalts from Sierra de San Bernardo (Patagonia, Chubut, Argentina). Geol. Mag. 145 (5), 714–732.
Cande, S., Leslie, R., 1986. Late Cenozoic tectonics of the southern Chile Trench. J. Geophys. Res. 91 (B1), 471–496.
Cembrano, J., Lara, L., 2009. The link between volcanism and tectonics in the southern volcanic zone of the Chilean Andes: a review. Tectonophysics 471, 96–113.
Ciciarelli, M., 1990. Análisis Estructural del Sector Oriental del Macizo Nordpatagónico y su significado metalogenético. Facultad de Ciencias Naturales y Museo, La Plata. PhD Thesis N° 555.
Coira, B., Franchi, M., Nullo, F., 1975. Vulcanismo del Terciario al oeste de Somuncura y su relación con el arco magmático de la Cordillera Nordpatagónica, Argentina. IV Congreso Geológico Chileno. Actas 4, 68–88. Antofagasta.
Conrad, C.P., Wu, B., Smith, E.I., Bianco, T.A., Tibbetts, A., 2010. Shear-driven upwelling induced by lateral viscosity variations and asthenospheric shear: a mechanism for intraplate volcanism. Phys. Earth Planet. Interior 178, 162–175.
Cucchi, R., Busteros, A., Lema, H., 2001. Hoja Geológica 4169 II, Los Menucos, Provincia de Río Negro. IGRM-SEGEMAR. Boletín 265, 67.
Chen, J.C., 1971. Petrology and chemistry of garnet lherzolite nodules in kimberlite from South Africa. Am. Min. 56, 2098–2110.
De Min, A., 1993. Il magmatismo Mesozoico K-alcalino del Paraguay Orientale: aspetti petrogenetici ed implicazioni geodinamiche. Universitá di Trieste, p. 242. Ph.D. Thesis.
DeMets, C., Gordon, R., Argus, D., Stein, S., 1990. Currunt plate motions. Geophys. J. Int. 101, 425–478.
D'Orazio, M., Agostini, S., Mazzarini, F., Innocenti, F., Manetti, P., Haller, M., Lahsen, A., 2000. The Pali Aike volcanic field, Patagonia: slab-window magmatism near the tip of South America. Tectonophysics 321, 407–427.
de Ignacio, C., López, I., Oyarzun, R., Márquez, A., 2001. The northern Patagonia Somuncura plateau basalts: a product of slab-induced, shallow asthenospheric upwelling ? Terra Nova 13, 117–121.

Folguera, A., Introcaso, A., Giménez, M., Ruiz, F., Martinez, P., Tunstall, C., Morabito, E., Ramos, V., 2007. Crustal attenuation in the Southern andean retroarc (38°–39°30′S) determined from tectonic and gravimetric studies: the Lonco-Luán asthenospheric anomaly. Tectonophysics 439, 129–147.
Folguera, A., Bottesi, G., Zapata, T., Ramos, V., 2008. Crustal collapse in the Andean backarc since 2 Ma: Tromen volcanic plateau, Southern Central Andes (36°40′-37°30′S). Tectonophysics 459, 140–160.
González, P., Coluccia, A., Franchi, M., 2003. Hoja 4169-III Ingeniero Jacobacci, Carta Geológica de la República Argentina, escala 1:250.000, Ingeniero Jacobacci 4169-III. Servicio Geológico Minero Argentino, Buenos Aires.
Green, D.H., 1970. A review of experimental evidence on the origin of basaltic and nephelinitic magmas. Phys. Earth Planet. Inter. 3, 221–235.
Gorring, M., Kay, S., Zeitler, P., Ramos, V., Rubiolo, D., Fernández, M., 1997. Neogene Patagonian plateau lavas: continental magmas associated with ridge collision at the Chile Triple Junction. Tectonics 16, 1–17.
Gorring, M.L., Kay, S.M., 2000. Carbonatite metasomatised peridotite xenoliths from southern Patagonia: implications for lithospheric processes and Neogene plateau magmatism. Contrib. Mineral. Petrol. 140, 55–72.
Gorring, M.L., Kay, S.M., 2001. Mantle processes and source of Neogene slab window magmas from Southern Patagonia, Argentina. J. Petrol. 42, 1067–1094.
Gorring, M.L., Singer, B., Gowers, J., Kay, S.M., 2003. Plio-Pleistocene basalts from the Meseta del Lago Buenos Aires, Argentina: evidence for asthenosphere-lithosphere interactions during slab window magmatism. Chem. Geol. 193, 215–235.
Haller, M., Massaferro, G., Meister, C., Prez, H., Carrasco, M., 2008. Volcanismo Basáltico del Neógeno tardío en el norte de Patagonia. 17 Congreso Geológico Argentino. Actas III, 1359–1360. San. Salvador Jujuy.
Haller, M., Pécskay, Z., Németh, K., Gméling, K., Massaferro, G., Meister, C., Nullo, F., 2009. Preliminary K-Ar Geochronology of Neogene Back Arc Volcanism in Northern Patagonia, Argentina. Third International Maar Conference, Malargüe. Abstracts: 40–41.
Hanson, G.N., 1978. The application of trace elements to the petrogenesis of igneous rocks of granitic composition. Earth Planet. Sci. Lett. 38, 26–43.
Hickey, R., Frey, F., Gerlach, D., Lopez, Escobar, 1986. Multiple sources for basaltic arc rocks from the southern volcanic zone of the andes (34–41°): trace element and isotopic evidence for contributions from subducted oceanic crust, mantle and continental crust. J. Geophys. Res. 91, 5963–5983.
Homovc, J.F., Conforto, G.A., Lafourcade, P.A., Chelotti, L.A., 1995. Fold Belt in the San Jorge Basin, Argentina: an example of tectonic inversion. In: Buchanan y, J.G., Buchanan, P.G. (Eds.), En Basin Inversion, vol. 88. Geological Society Special Publication, pp. 235–248.
Irvine, T.N., Baragar, W.R.A., 1971. A guide to the chemical classification of the common volcanic rocks. Can. J. Earth Sci. 8, 523–548.
Kay, S.M., Copeland, P., 2006. Early to middle Miocene back-arc magmas of the Neuquén Basin of the southern Andes: geochemical consequences of slab shallowing and the westward drift of South America. In: Kay, S.M., Ramos, V.A. (Eds.), Evolution of an Andean Margin: a Tectonic and Magmatic Perspective from the Andes to the Neuquén Basin (35°–39° S Lat.). Geological Society of America, pp. 185–213. Special Paper 407.
Kay, S., Ardolino, A., Franchi, M., Ramos, V., 1993. Origen de la meseta de Somun Cura: distribución y geoquímica de sus rocas volcánicas máficas. XII Congreso Geológico Argentino. Actas 4, 236–248. Buenos Aires.
Kay, S.M., Gorring, M., Ramos, V., 2004. Magmatic sources, setting and causes of Eocene to Recent Patagonian plateau magmatism (36°S to 52°S latitude). Rev. la Asoc. Geológica Argent. 59 (4), 556–568.
Kay, S.M., Burns, W.M., Copeland, P., Mancilla, O., 2006. Upper Cretaceous to Holocene magmatism and evidence for transient Miocene shallowing of the Andean subduction zone under the northern Neuquén basin. In: Kay, S.M., Ramos, V.A. (Eds.), Evolution of an Andean Margin: a Tectonic and Magmatic View from the Andes to the Neuquén Basin (35°–39°S lat.). Geological Society of America Special Paper 407, pp. 19–60.
Le Bas, M.J., Le Maitre, R.W., Strekeisen, A., Zanetin, B., 1986. A chemical classification of volcanic rock base on the total alkali-silica diagram. J. Petrol. 27, 745–750.
Lin, S.-C., 2014. Three-dimensional mantle circulations and lateral slab deformation in the southern Chilean subduction zone. J. Geophys. Res. Solid Earth 119. http://dx.doi.org/10.1002/2013JBO10846.
MacGregor, I.D., 1974. The system $MgO–Al_2O_3–SiO_2$: solubility of Al_2O_3 in enstatite for spinel and garnet peridotite compositions. Am. Mineral. 59, 110–119.
Mahlburg Kay, S., Ardolino, A., Gorring, M., Ramos, V., 2007. The Somuncura large igneous Province in Patagonia: Interaction of a transient mantle Thermal anomaly with a subducting slab. J. Petrol. 48 (1), 43–77.
Massaferro, G.I., Alric, V.I., Haller, J.F., 2002. El campo volcánico cuaternario del Basalto Cráter en la Patagonia Septentrional. XV Congreso Geológico Argentino. Actas II, 91–96. Actas CD-ROM, 193 pdf, 6 pp. El Calafate.
Massaferro, G.I., Haller, M.J., D'Orazio, M., Alric, V.I., 2006. Sub-recent volcanism in Northern Patagonia: a tectonomagmatic approach. J. Volcanol. Geotherm. Res. 155, 227–243.
Massaferro, G., Haller, M., Dostal, J., 2010. Modelos de Cristalización Fraccionada para basaltos Plio-pleistocenos de la Patagonia septentrional: ¿Una fuente común? 10° Congreso de Mineralogía y Metalogenia. Actas, 307–310. Río Cuarto.
McKenzie, D., O'Nions, R.K., 1991. Partial melt distributions from inversion of rare Earth element concentrations. J. Petrol. 32, 1,021–1,091.
Müller, R.D., Roest, W.R., Royer, J.-Y., Gahagan, L.M., Sclater, J.G., 1997. Digital isochrons of the world's ocean floor. J. Geophys. Res. 102, 3211–3214. http://dx.doi.org/10.1029/96JB01781.
Muñoz, J., Troncoso, R., Duhart, P., Crignola, P., Farmer, L., Stern, C., 2000. The relation of the mid-Tertiary coastal magmatic belt in south-central Chile to the late Oligocene increase in plate convergence rate. Revista. Geológica Chile 27 (2), 177–203.
Nakamura, N., 1974. Determination of REE, Ba, Fe, Mg, Na, and K in carbonaceous and ordinary chondrites. Geochim. Cosmochim. Acta 38, 757–775.
Norabuena, E., Leffler-Griffin, L., Mao, A., Dixon, T., Stein, S., Sacks, S., Ocola, L., Ellis, M., 1998. Space geoditic observations of Nazca-South America convergence across the Central Andes. Science 279, 358–362.
Nullo, F., 1978. Descripción geológica de la Hoja 41d Lipetrén, Provincia de Río Negro. Boletín N° 158. Servicio Geológico Nacional.
Nullo, F., 1983. Descripción geológica de la Hoja 45c Pampa de Agnia. Provincia del Chubut. Boletín N° 199. Servicio Geológico Nacional.
Pearce, T.H., 1978. Olivine fractionation equations for basaltic and ultrabasic liquids. Nature 276, 771–774.
Pécskay, Z., Molnár, F., 2002. Relationships between volcanism and hydrothermal activity in the Tokaj Mountains, Northern Hungary, based on K/Ar. Geol. Carp. 53 (5), 1–12.
Pécskay, Z., Haller, M.J., Németh, K., 2007. Preliminary K/Ar geochronology of the crater Basalt volcanic field (CBVF), Northern Patagonia. Rev. la Asoc. Geológica Argent. 62 (1), 25–29.
Ramos, V., Kay, S., 1992. Southern Patagonian plateau basalts and deformation: backarc testimony of ridge collisions. Tectonophysics 205, 1–20.
Ravazzoli, I., Sessana, F., 1977. Descripción geológica de la hoja 41c, Río Chico, pcia. de Río Negro. Boletín N° 148. Servicio Geológico Nacional.
Remesal, M., 1988. Geología y petrología de los basaltos de la Meseta de Somuncurá. University of Buenos Aires, p. 207. PhD. Thesis.
Remesal, M., Salani, F., Cerredo, M.E., 2012. Petrología del Complejo Volcánico Barril Niyeu (Mioceno inferior), Patagonia Argentina. Rev. Mex. Ciencias Geológicas 29 (2), 463–477.
Ringwood, A.E., 1966. The chemical composition and origin of the Earth. In: Hurley, P.M. (Ed.), Advances in Earth Science: Contributions to the International Conference on the Earth Sciences. MIT Press, MA, pp. 287–356. Cambridge.
Rivalenti, G., Mazzucchelli, M., Laurora, A., Ciuffi, S., Zanetti, A., Vannucci, R., Cingolani, C., 2004. The backarc mantle lithosphere in Patagonia, South America. J. South Am. Earth Sci. 17, 121–152.
Søager, N., Holm, P.M., Llambías, E.J., 2013. Payenia volcanic province, southern Mendoza, Argentina: OIB mantle upwelling in a backarc invironment. Chem. Geol. 349-350, 36–53.
Somoza, R., 1998. Updated Nazca (Farallon) – south America relative motions during the last 40 Ma: implications for mountain building in the Central Andean region. J. South Am. Earth Sci. 11, 211–215.
Stern, C.R., Frey, F.A., Futa, K., Zartman, R.E., Peng, Z., Kyser, T.K., 1990. Trace element and Sr, Nd, Pb, and O isotopic composition of Pliocene and Quaternary alkali basalts of the Patagonian Plateau lavas of southernmost South America. Contrib. Mineral. Petrol. 104, 294–308.
Stormer, J.C., Nicholls, J., 1978. XLFRAC: a program for interactive testing of magmatic differentiation models. Comput. Geosci. 4, 143–159.
Sun, S.S., McDonough, W.F., 1989. Chemical and isotopic systematics of oceanic basalts: implications for mantle composition and processes. In: Saunders, A.D., y Norry, M.J. (Eds.), Magmatism in Ocean Basins. Geol. Soc., London, pp. 313–345. Spec. Pub. 42.
Sylwan, C., 2001. Geology of the Golfo San Jorge Basin, Argentina. J. Iber. Geol. 27, 123–157.
Takahashi, E., Kushiro, I., 1983. Melting of a dry peridotite at high pressure and basalt magma series. Am. Mineral. 68, 859–879.
Tassara, A., Yañez, G., 2003. Relación entre el espesor elástico de la litosfera y la segmentación tectónica del margen andino (15–47°S). Rev. Geol. Chile 30 (2), 159–186.
Tašárová, Z., 2007. Towards understanding the lithospheric structure of the southern Chilean subduction zone (36°S–42°S) and its role in the gravity field. Geophys. J. Int. 170, 995–1014.
White, W.M., 2013. Geochemistry. Wiley and Blackwell, p. 637.
Wyllie, P.J., 1981. Plate tectonics and magma genesis. Geol. Rundsch. 70, 128–153.
Zaffarana, C., Lagorio, S., Somoza, R., 2012. Palemagnetism and geochemistry from the Upper cretaceous Tres Picos Prieto locality (43°S), Patagonian plateau basalts. Andean Geol. 39 (1), 53–66.
Zindler, A., Hart, S., 1986. Chemical geodynamics. Annu. Rev. Earth Planet. Sci. 14, 493–571.